Available online at www.sciencedirect.com
ScienceDirect
Intermetallics 15 (2007) 791–795
Intermetallics
www.elsevier.com/locate/intermet

# The characterization of plastic deformation in Ce-based bulk metallic glasses

L.C. Zhang [a], B.C. Wei [a,*], D.M. Xing [b], T.H. Zhang [b], W.H. Li [a], Y. Liu [a]

[a] National Microgravity Laboratory, Institute of Mechanics, Chinese Academy of Sciences, Beijing 100080, China
[b] State Key Laboratory of Nonlinear Mechanics (LNM), Institute of Mechanics, Chinese Academy of Sciences, Beijing 100080, China
Available online 13 November 2006

**Abstract**

The plastic deformation behavior of $Ce_{68}Al_{10}Cu_{20}Nb_2$ and $Ce_{70}Al_{10}Cu_{20}$ bulk metallic glasses (BMGs) at room temperature was studied by depth-sensing nanoindentation and microindentation. It is shown that the two BMGs exhibit a continuous plastic deformation without distinct serration at the all of the studied loading rates during nanoindentation. An obvious creep displacement was observed during the holding-load segment at the maximum load for the two alloys, and the magnitude of creep during holding-load increases with loading rate. The subsurface plastic deformation zone of the two BMGs after indentation at various loading rates was investigated through bonded interface technique using depth-sensing microindentation. A highly developed shear banding pattern can be observed in the plastic deformation region, though the global load–depth curves illuminate a ''homogeneous flow''. The plastic deformation behavior of the Ce-based BMGs during indentation measurements is discussed in terms of localized viscous flow.


*Keywords:* B. Glasses, metallic; B. Plastic deformation mechanisms; B. Creep

## 1. Introduction

The plastic deformation of metallic glasses is classified as homogeneous or inhomogeneous [1–4]. Homogeneous flow occurs at low imposed strain rates and at temperatures near and above the glass transition ($T > 0.7T_g$). In this regime, every element of the metallic glass contributes to the overall plastic strain. At ambient temperature or at large imposed strain rates, plastic flow becomes inhomogeneous and tends to localize on a small number of bands that form approximately on maximum shear stress planes. More recently, Ce-based bulk metallic glasses (BMGs) with an exceptionally low glass transition temperature $T_g$ have been reported. These materials can be repeatedly shaped in near-boiling water, and can thus be regarded as ''metallic plastics'' [5,6]. Room temperature is about $0.8T_g$ for the Ce-based BMGs. This provides an opportunity for the study of homogeneous plastic deformation in BMGs at room temperature. However, no distinct overall plastic strain can be observed during the quasi-static state uniaxial compressive tests [5], which indicate a strongly inhomogeneous deformation. For further understanding the plastic flow mechanism in Ce-based BMGs, detailed studies on the plastic deformation process are needed. Nanoindentation has recently been proposed as a key method for the study of plastic deformation behaviors in BMGs [7–13]. Nanoindentation tests allow considerably larger plastic deformation to be accumulated in the quasi-brittle materials in a localized area around the indented regions. In this work, the deformation behavior and the loading rate effect on deformation features in two Ce-based BMGs are investigated by nanoindentation. Furthermore a direct observation of the plastic deformation region is proved for understanding the deformation mechanism in the Ce-based BMGs.

## 2. Experimental

Cylindrical rods with 2 mm in diameter of the nominal chemical composition $Ce_{68}Al_{10}Cu_{20}Nb_2$ and $Ce_{70}Al_{10}Cu_{20}$

* Corresponding author. Tel.: +86 10 62614945; fax: +86 10 62615524.
*E-mail address:* weibc@imech.ac.cn (B.C. Wei).

0966-9795/$ - see front matter © 2006 Elsevier Ltd. All rights reserved.
doi:10.1016/j.intermet.2006.10.009

BMGs were prepared by melting pure metals in an argon atmosphere and then chill-casting in a copper mould. The structure of the samples was characterized by X-ray diffraction (XRD) using a Philips PW 1050 diffractometer using Cu $K_\alpha$ radiation. Thermal analysis was performed using a Perkin–Elmer DSC-7 differential scanning calorimeter under argon atmosphere. A constant heating rate of 0.33 K/s was employed. The specimens for nanoindentation measurements were mechanically polished to a mirror finish and tested in an MTS Nano Indenter® XP with a Berkovich diamond tip (the tip radius is about 50 nm). Fused silica was used as a reference sample for the initial tip calibration procedure. The indentations were performed in load-control mode to a depth limit of 1 μm using loading rates from 0.03 to 1.0 mN/s. The maximum load was held constant for 10 s, and then was unloaded at the rates as same as the loading one. The thermal drift of the instrument was maintained below 0.05 nm/s. At least six indentations were made for each test. All tests were carried out at 396 K. The study of subsurface deformation morphology was obtained through the bonded interface technique [14]. The two mirror polished surfaces were bonded using a high strength adhesive. A careful bonding was made to minimize the bond layer thickness ensuring the bonded layer thickness for different specimen is almost same. The microindentation tests were performed using Vickers' indenter on the bonded interface as well as away from it. The indenter is attached to a load cell that is bolted to the bottom of the crosshead of an Instron 5848 Microforce Tester. The indentation measurements were performed in displacement-control mode to a load limit of 10 N. It was also ensured that one of the indentation diagonals coincides with the interface. Indents' surface and subsurface observations were performed using a Neophot-21 optical microscope.

## 3. Results and discussion

Fig. 1 demonstrates the DSC traces of the two Ce-based BMGs at a constant scanning rate of 0.33 K/s. The onset temperature of the glass transition ($T_g$), the crystallization temperature ($T_x$) and supercooled liquid region ($\Delta T_x = T_x - T_g$) is 359.1 K, 412.2 K and 53.1 K for $Ce_{68}Al_{10}Cu_{20}Nb_2$ BMG, and 356.9 K, 400.6 K and 43.7 K for $Ce_{70}Al_{10}Cu_{20}$ BMG, respectively. These values agree with the results given in Ref. [6]. The ratio of room temperature over $T_g$ is almost the same of about 0.83 for the two BMGs. The inset in Fig. 1 exhibits the XRD patterns of as-cast $Ce_{68}Al_{10}Cu_{20}Nb_2$ and $Ce_{70}Al_{10}Cu_{20}$ alloys. All the as-cast alloys exhibit XRD spectrum typical for amorphous phase without obvious crystalline peak.

Typical load–depth ($P$–$h$) curves during nanoindentation at various loading rates of the two BMGs are presented in Fig. 2, where the samples are indented to the depth of 1000 nm. The origin of each curve has been horizontally displaced for clearer observation. It can be seen that the $P$–$h$ curves of the two BMGs at all loading rates do not exhibit distinct serrated flow during the loading process. This is in contrast to the deformation behavior of other BMGs, e.g.

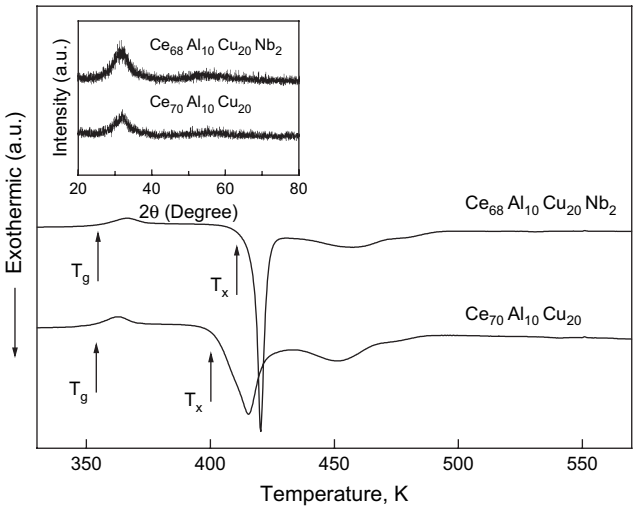


Fig. 1. DSC curves for the as-cast $Ce_{68}Al_{10}Cu_{20}Nb_2$ and $Ce_{70}Al_{10}Cu_{20}$ BMGs at a heating rate of 0.33 K/s. The inset is XRD patterns for the two alloys.

Zr-, Pd-, and Mg-based BMGs during nanoindentation, where a pronounced serrated flow has been observed at least at low loading rates [7–12]. It can also be found in Fig. 2 that the maximum load at the indentation depth of 1000 nm increases

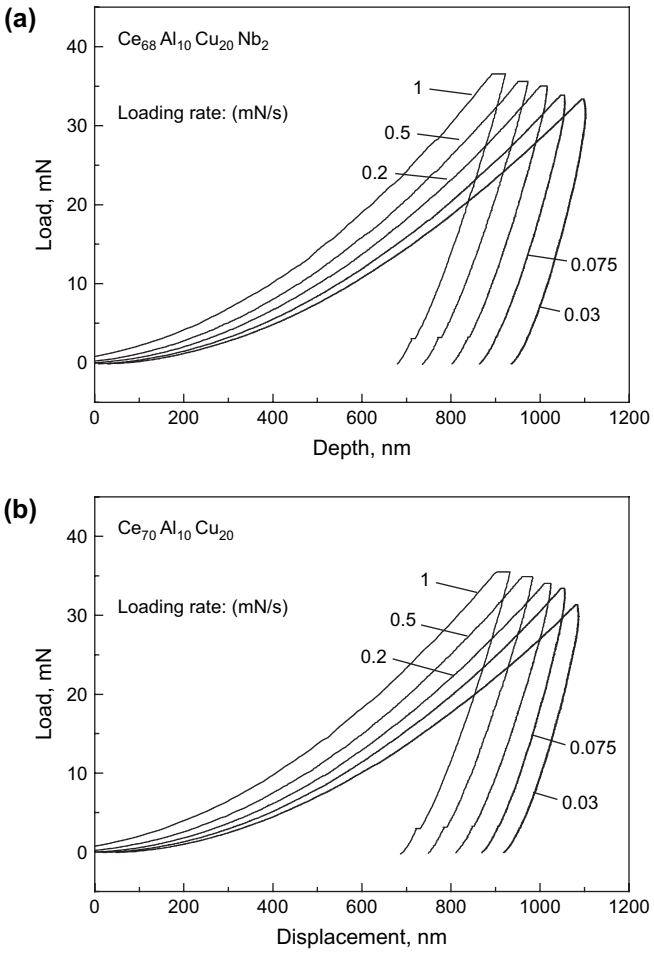


Fig. 2. Typical load–depth ($P$–$h$) curves for the two BMGs during nanoindentation at various loading rates. (a) $Ce_{68}Al_{10}Cu_{20}Nb_2$; (b) $Ce_{70}Al_{10}Cu_{20}$.

with increasing loading rate for the two BMGs. This means that the hardness of the Ce-based BMGs at room temperature increases with the loading rate. The hardness value is almost the same for the two BMGs at all the loading rates, that is, about 1.3 GPa at 0.03 mN/s and 1.8 GPa at 1.0 mN/s. Whereas, hardness is normally independent of the loading rate at room temperature for other BMGs [7,15].

It should be noted from the $P-h$ curves (Fig. 2) that during the hold segment for 10 s at the maximum load, a creep displacement could clearly be observed in the two BMGs. The magnitude of the creep displacement during holding-load depends strongly on the loading rate, i.e. higher loading rates promote larger creep displacement for the two BMGs. At the same loading rate, two BMGs exhibit a similar creep displacement, e.g. about 28 nm at 1 mN/s.

Generally, homogeneous deformation in metallic glasses takes place at high temperatures ($>0.70\ T_g$), in contrast to inhomogeneous deformation at ambient temperature. The plastic deformation in metallic glasses at room temperature is concentrated in the narrow regions called shear bands [16]. Serrated flow phenomenon manifested as a stepped load–displacement curve punctuated by discrete bursts of plasticity during nanoindentation was already found in Pd-, Zr-, Nd- and Mg-based BMGs [7–12]. The serrations correspond to the activation of individual shear bands. Low indentation rates promote more pronounced serrations, as a single shear band could propagate adequately at low loading rates. The $P-h$ curves for the present two BMGs do not exhibit distinct serrations at all the studied loading rates. This may suggest that the Ce-based BMGs deform homogeneously during nanoindentation at room temperature. However, the strain rate sensitivity coefficient ($m$) of the two Ce-based BMGs during the plastic deformation at room temperature is quite low and in the order of $10^{-2}$ [17]. It is well known that $m = 1$ indicates a Newtonian flow, and $m < 1$ for non-Newtonian flow. The quite low $m$ values here indicate a highly localized plastic deformation for the present two alloys. To further illuminate the plastic deformation feature of the Ce-based BMGs, we studied the morphology of plastic deformation region around the indent after microindentation.

Fig. 3 demonstrates the typical subsurface and upper surface plastic deformation morphologies of the $Ce_{68}Al_{10}Cu_{20}Nb_2$ BMG after indentation at different loading rates. A highly developed shear band pattern could be observed in the subsurface plastic deformation region at all loading rates (Fig. 3a,c). The deformation zone is semi-circular in nature containing two types of shear bands; those are semi-circular and radial shear bands. A number of incomplete circular patterns of shear bands are also observed in the pile-up area around the indents (Fig. 3b,d). They represent the overlapping layers of displaced material that flow upwards and away from the depth of the indents. Fig. 4 shows the typical subsurface and upper surface plastic deformation morphologies of the $Ce_{67}Al_{10}Cu_{20}$ BMG. Many shear bands are also observed underneath the indent (Fig. 4a,c) and around the indent surface (Fig. 4b,d). By comparing the shear band feature of the alloy at different loading rates, we can find that the number of shear bands is higher at low loading rates than that at higher loading rates (Figs. 3 and 4). This is in contrast to the results in Zr- and

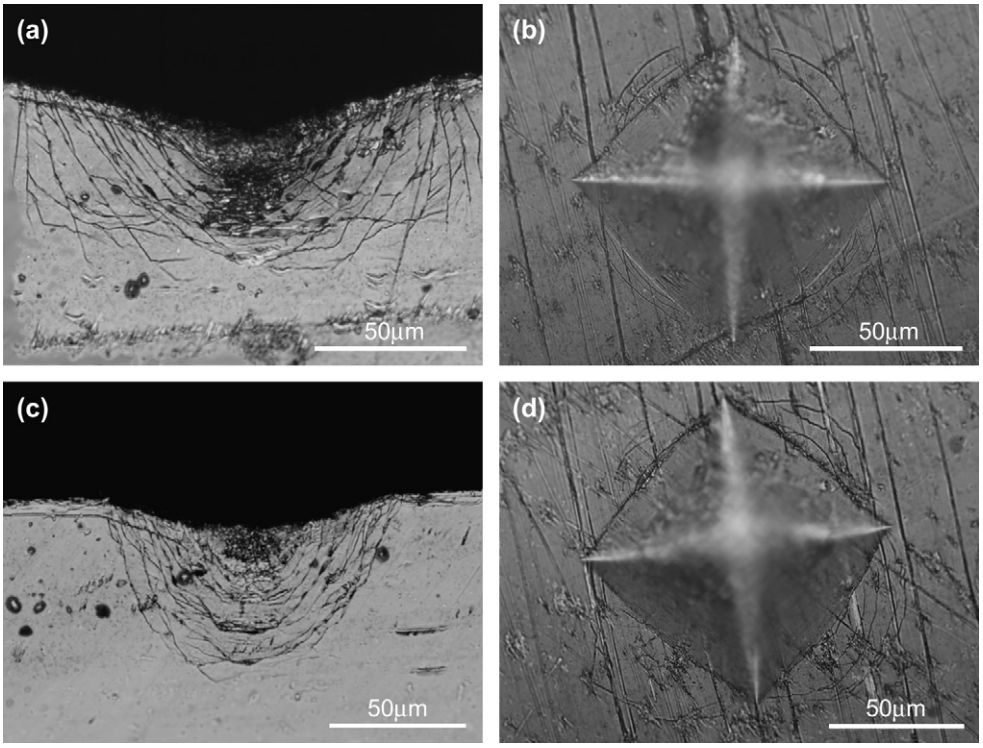


Fig. 3. Plastic deformation region morphology for $Ce_{68}Al_{10}Cu_{20}Nb_2$ BMG after indentation at different loading rates. (a) 15 nm/s, underneath indent; (b) 15 nm/s, around indent; (c) 1000 nm/s, underneath indent; (d) 1000 nm/s, around indent.

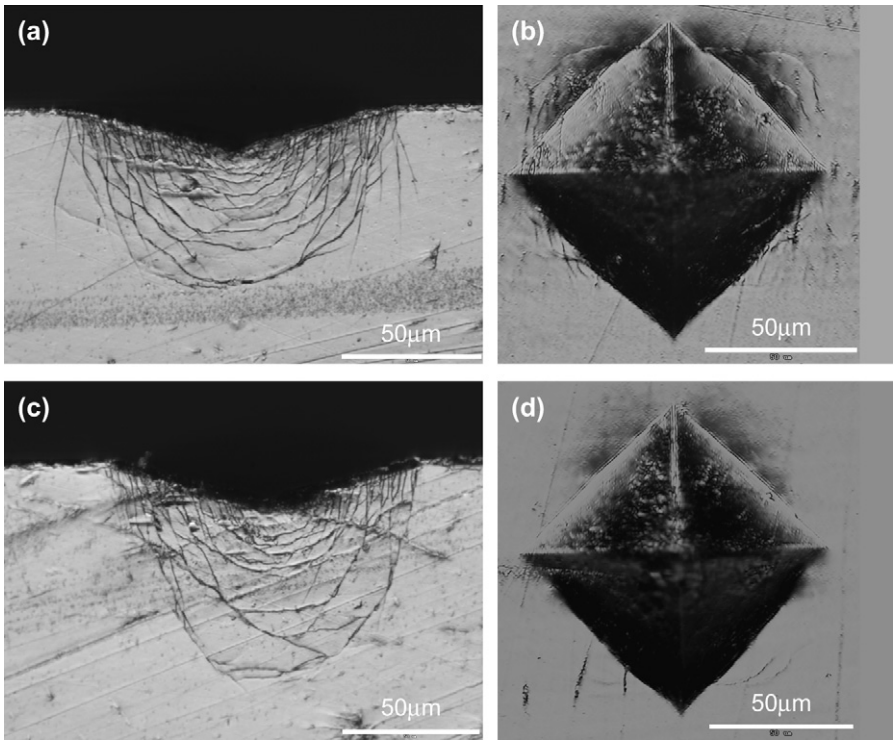


Fig. 4. Plastic deformation region morphology for $Ce_{70}Al_{10}Cu_{20}$ BMG after indentation at different loading rates. (a) 15 nm/s, underneath indent; (b) 15 nm/s, around indent; (c) 1000 nm/s, underneath indent; (d) 1000 nm/s, around indent.

Mg-based BMGs, where more shear bands were observed at higher loading rates [12].

The morphology of the plastic deformation region in the two BMGs after indentation exhibits a distinct inhomogeneous deformation feature characterized by forming shear bands. Furthermore, it should be pointed that the size of the shear band upsets in the two BMGs is much larger than that in Zr-based BMG at the same indentation condition [12]. This should lead to a pronounced serrated flow during indentation, as the propagation of an individual thick shear band will cause a strongly rigid slip of the surrounding elastically deformed materials. However, there is no obvious serration in the $P-h$ curves of the two BMGs during nanoindentation at various loading rates (Fig. 2). The disappearance of serration should be related to the local viscous flow of the Ce-based BMGs during indentation. It has been shown in Fig. 2 that creep takes place during loading process, which contains viscoelastic viscoplastic flow. The creep occurs preferentially in the maximum shear stress direction prior to the appearance of shear bands, and will relax the stress concentration. Moreover, the localized viscous flow around the shear bands will accommodate the rigid displacement of the materials caused by the propagation of shear bands. These two factors give rise to a continuous plastic deformation in Ce-based BMGs during indentation.

## 4. Summary

The plastic deformation behavior of $Ce_{68}Al_{10}Cu_{20}Nb_2$ and $Ce_{70}Al_{10}Cu_{20}$ bulk metallic glasses (BMGs) at room temperature was studied by depth-sensing nanoindentation and microindentation. The two BMGs exhibit a continuous plastic deformation without distinct serration at the all of the studied loading rates during nanoindentation. However, the plastic deformation region underneath and around the indents after indentation measurements shows a highly developed shear band pattern, indicating a highly inhomogeneous flow. The localized creep deformation prior to the appearance of shear band is thought to be the reason for the disappearance of serration during indentation.

## Acknowledgements

The authors would like to acknowledge the financial support provided by National Nature Science Foundation of China (Grant Nos. 50571109, 10372103 and 10432050) and the Knowledge Innovation Program of Chinese Academy of Sciences.

## References

[1] Spaepen F. Acta Metall 1977;25:407.
[2] Wang WH, Dong C, Shek CH. Mater Sci Eng R 2004;44:45.
[3] Flores KM, Dauskardt RH. Intermetallics 2004;12:1025.
[4] Nishiyama N, Kato H, Saida J, Inoue A, Chen HS. Jpn J Appl Phys 2002;41:741.
[5] Zhang B, Zhao DQ, Pan MX, Wang WH, Greer AL. Phys Rev Lett 2005;94:205502.
[6] Zhang B, Wang RJ, Zhao DQ, Pan MX, Wang WH. Phys Rev B 2004;70:224208.
[7] Schuh CA, Nieh TG. J Mater Res 2004;19:46.
[8] Schuh CA, Nieh TG. Acta Mater 2003;51:87.

[9] Schuh CA, Argon AS, Nieh TG, Wadsworth J. Philos Mag A 2003;83:2585.
[10] Jiang WH, Atzmon M. J Mater Res 2003;18:755.
[11] Wei BC, Zhang TH, Li WH, Sun YF, Yu Y, Wang YR. Intermetallics 2004;12:1239.
[12] Li WH, Zhang TH, Xing DM, Wei BC, Wang YR, Dong YD. J Mater Res 2006;21:75.
[13] Greer AL, Walker IT. Mater Sci Forum 2002;77:386.
[14] Ramamurty U, Jana S, Kawamura Y, Chattopadhyay K. Acta Mater 2005;53:705.
[15] Mukai T, Nieh TG, Kawamura Y, Inoue A, Higashi K. Scripta Mater 2002;46:43.
[16] Bian Z, He G, Chen GL. Scripta Mater 2002;46:407.
[17] Wei BC, Zhang TH, Li WH, Xing DM, Zhang LC, Wang YR. Mater Trans 2005;46:2959.